# Quartz Transducer Modeling for Development of BAW Resonators

Leonardo B. M. Silva and Edval J. P. Santos
Laboratory for Devices and Nanostructures, Departamento de Eletrônica e Sistemas,
Universidade Federal de Pernambuco. Rua Acadêmico Hélio Ramos, s/n, Várzea, 50740-530, Recife, PE, Brasil. Email: edval@ee.ufpe.br, Ph./Fax: +55(81)2126-8214

**Abstract:** Transducer optimization is a key aspect for successful development and deployment of advanced sensors, especially when designing 3D structures for harsh environments. For piezoelectric transducers, plate thickness determines the operating frequency of the resonator, which is frequently tuned in the shear thickness vibration mode. Quartz has been the material of choice for the fabrication of bulk acoustic wave (BAW) devices, which are used for measurement of many quantities, such as, temperature, pressure, acceleration, mass. All the required steps to simulate the shear thickness vibration mode for quartz bulk acoustic wave (BAW) devices are presented in both, two and three dimensions. Different crystal cuts are analyzed, including the AT-cut. The simulation was carried out with COMSOL Multiphysics version 4.2a.

**Keywords:** BAW resonators, quartz, shear thickness vibration mode, susceptance, frequency resonance.

## 1. Introduction

Piezoelectric resonators are widely used for building sensors, including advanced sensor for harsh environments. Physical quantities, such as, temperature, pressure, acceleration, mass, can be measured as an electrical signal, due to the piezoelectric effect. Many different modes of vibration can be excited such as bending, torsional, extension, buckling, shear, and lateral. In general each of these modes dominates at a given frequency and it is possible to tune the electronic circuit to operate in a specific transducer vibration mode. The resonator body vibrates, and its vibration is affected by the environment. An electric quantity, charge or frequency, proportional to the physical quantity change [1,2].

Bulk acoustic wave (BAW) devices made of quartz is an industry standard. Depending on the application, the quartz blank is cut with a selected orientation. Crystal orientation is chosen based upon desired behavior, such as frequency × temperature or frequency × pressure

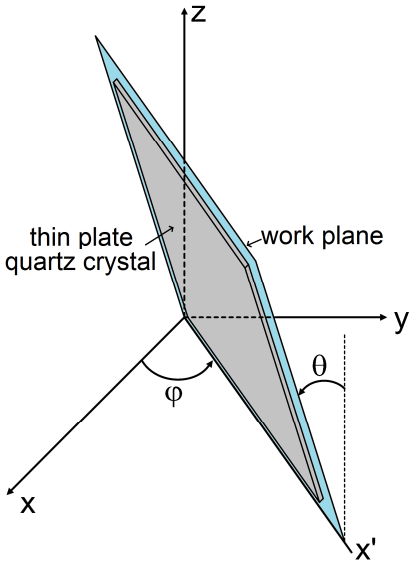


**Figure 1**. Double rotated cut angles for a blank quartz. The coordinate system is equivalent to the default COMSOL system. The displacements occur in the x'-direction.

characteristics. The quartz crystal is cut in the form of thin plate, and typically for frequencies in the MHz range, the shear thickness vibration mode is selected. In such vibration the whole transducer body moves, hence the name Bulk Acoustic Wave (BAW) resonator. The plate thickness determines the vibration frequency, and hence the operating frequency of the electronic circuit attached to it. The most commonly used types of quartz resonators in the shear thickness vibration mode are the AT-cut and SC-cut, due to its very good frequency stability. For the AT-cut, the orientation angles are are $\theta = 35.25°$ and $\varphi = 0°$ [3], as shown in Figure 1.

The piezoelectric behavior can be modeled using the finite element method [4,5,6,7]. In this paper, COMSOL Multiphysics version 4.2a is used to simulate different crystal cuts and transducer geometries. It can help to generate a satisfactory transducer specification. To simulate a quartz BAW resonator, different settings can be defined. For the purpose of demonstration of the use of the software, this investigation is carried out neglecting the damping factor and the

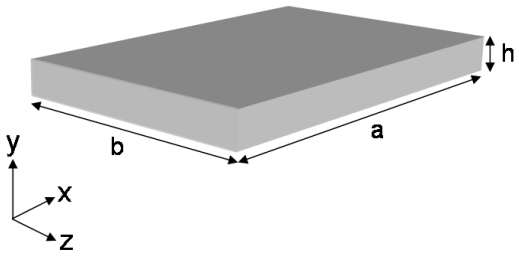


**Figure 2**. Arrangement to verify the vibration in a piezoelectric plate. The bottom and top surfaces are subjected to an electric potential.

effect of the electrodes thickness on the resonance frequency. The damping factor is related to the losses of the structure. Differents meshes, 2D and 3D, singles and double rotations, resonance frequency up to fifth harmonic for shear vibration mode, extraction of equivalent circuit parameters and estimation of the quality factor are examined.

The paper is organized as follows. This introduction is the first section. In section 2, a summary of theory of piezoelectric is presented. In section 3, the use of the COMSOL is described, where key aspects of the simulation steps are discussed. The four section presents the results and analysis. Finally, the conclusions in section 5.

## 2. Piezoelectric Theory

Quartz crystal is a weak piezoelectric material, it has low piezoelectric coupling coefficient. Hence, electrical and mechanical coupling can be approximated by linear relations. The piezoelectric coupling can be represented mathematically through the constitutive relations of piezoelectricity, as given by Equations 1 and 2, in Einstein notation. These equations represent the direct and reverse effect, respectively.

$$D_i = e_{ijk} S_{jk} + \varepsilon_{ij} E_j \tag{1}$$

$$T_{ij} = c_{ijkl} S_{kl} - e_{kij} E_k \tag{2}$$

where $D$ is the electric displacement vector, $e$ is the piezoelectric coupling matrix, $S$ is the strain matrix, $\varepsilon$ is the relative permittivity matrix, $E$ is the applied electric field vector, $T$ is the stress matrix, and $c$ is the elasticity or elastic stiffness matrix.

Typically, the transducer is a plate. Although many vibration modes are possible, for

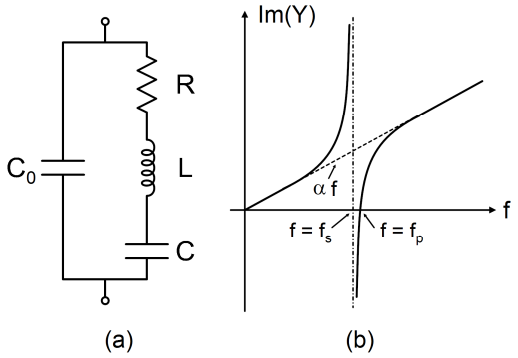


**Figure 3**. (a) Electrical equivalent circuit for quartz crystal resonator. (b) Serie and parallel frequencies in the imag(Admittance) curve characteristic.

frequencies in the MHz range, it is designed to vibrate in the shear thickness mode [8].

Should the surfaces parallel to the y- and z-planes be fixed (see Figure 2) so that displacements $u_y$ and $u_z$ are zero, it can be shown that the eigenfrequency equation for the harmonics is given by Equation 3, where $f_n$ is the frequency of $n$-th harmonic, $v$ is the shear acoustic wave speed and $h$ is the thickness of the plate. As the transducer is symmetric with respect to inversion, only odd values of $n$ lead piezoelectric coupling.

$$f_n = n\frac{v}{2h} \tag{3}$$

The acoustic speed for the quartz crystal in AT-cut is given by Equation 4.

$$v = \sqrt{\frac{\hat{c}_{66}}{\rho}} \tag{4}$$

where ρ is the material density and $\hat{c}_{66}$ is the elasticity constant.

The elasticity constant of a piezoelectric material is modified by the electromechanical coupling coefficient, $k_{26}^2$. In the $pq$ notation is given as shown in Equation 5.

$$\hat{c}_{66} = c_{66}\left(1 + k_{26}^2\right),\ k_{26}^2 = \frac{e_{26}^2}{c_{66}\varepsilon_{22}} \tag{5}$$

Near the resonance frequency the quartz resonator can be represented by an electrical equivalent circuit, as shown in Figure 3(a). Two resonance frequencies are present, the series-resonance, $f_s$, and the parallel-resonance, $f_p$, see Figure 3(b).

To reduce the coupling between the shear thickness mode and other modes such as, the

**Table 1:** Quartz crystal cuts, the angles are defined in Figure 1.

| θ(°) | φ(°) | cut |
|---|---|---|
| -60 | 0 | BC |
| -57 | 0 | FT |
| -49 | 0 | BT |
| 31 | 0 | AC |
| 35.25 | 0 | AT |
| 38 | 0 | CT |
| 42.75 | 0 | ST |
| 66.5 | 0 | ET |
| 35.25 | 21.9 | SC |

**Table 2:** Constants for AT-cut quartz [10].

| | |
|---|---|
| $[c]=$ | $\begin{bmatrix} 86.74 & -8.25 & 27.15 & -3.66 & 0 & 0 \\ -8.25 & 129.77 & -7.42 & 5.7 & 0 & 0 \\ 27.15 & -7.42 & 102.83 & 9.92 & 0 & 0 \\ -3.66 & 5.7 & 9.92 & 38.61 & 0 & 0 \\ 0 & 0 & 0 & 0 & 68.81 & 2.53 \\ 0 & 0 & 0 & 0 & 2.53 & 29.01 \end{bmatrix} \times 10^9$ N/m$^2$ |
| $[e]=$ | $\begin{bmatrix} 17.1 & -15.2 & -1.87 & 6.7 & 0 & 0 \\ 0 & 0 & 0 & 0 & 10.8 & -9.5 \\ 0 & 0 & 0 & 0 & -7.61 & 6.7 \end{bmatrix} \times 10^{-2}$ C/m$^2$ |
| $[\varepsilon]=$ | $\begin{bmatrix} 39.21 & 0 & 0 \\ 0 & 39.82 & 0.86 \\ 0 & 0.86 & 40.42 \end{bmatrix} \times 10^{-12}$ C/Vm |

flexural mode, it is also required to optimize the transducer lateral dimensions or diameter, *a*. Such coupling occurs at specific dimensions. Using Midlin plate theory, an optimum *a/h* ratio can be found. Varying *a/h* one can find dimensions of maximum coupling. Minimum coupling is set halfway between two maxima. In Equation 6, there is an expression for the AT-cut [9].

$$\frac{a}{h}=\left(m+\frac{1}{2}\right)1.6056,\ m=1,2,3\ldots M \qquad (6)$$

As mentioned previously, for frequencies in the range of 1 MHz to 10 MHz, the quartz transducer is designed to vibrate in the thickness shear mode. Thus the plate thicknesses are in the millimeter range. For the desired frequency × temperature or frequency × pressure characteristics, the crystal must be cut with a well defined orientation, examples of possible orientations for shear thickness vibration mode are listed in the Table 1. The angles are defined in Figure 1.

**Table 3:** Constants for left-handed quartz [10].

| | |
|---|---|
| $[c]=$ | $\begin{bmatrix} 86.74 & 6.99 & 11.91 & -17.91 & 0 & 0 \\ 6.99 & 86.74 & 11.91 & 17.91 & 0 & 0 \\ 11.91 & 11.91 & 107 & 0 & 0 & 0 \\ -17.91 & 17.91 & 0 & 57.94 & 0 & 0 \\ 0 & 0 & 0 & 0 & 57.94 & -17.91 \\ 0 & 0 & 0 & 0 & -17.91 & 39.88 \end{bmatrix} \times 10^9$ N/m$^2$ |
| $[e]=$ | $\begin{bmatrix} 17.1 & -17.1 & 0 & -4.06 & 0 & 0 \\ 0 & 0 & 0 & 0 & 4.06 & -17.1 \\ 0 & 0 & 0 & 0 & 0 & 0 \end{bmatrix} \times 10^{-2}$ C/m$^2$ |
| $[\varepsilon]=$ | $\begin{bmatrix} 39.21 & 0 & 0 \\ 0 & 39.21 & 0 \\ 0 & 0 & 41.03 \end{bmatrix} \times 10^{-12}$ C/Vm |

For each crystal cut, there is a set of constants for the elastic stiffness matrices *c*, piezoelectric matrix *e* and permittivity matrix $\varepsilon$. The elastic stiffness matrix for the quartz in the AT-cut can be seen in Table 2. To avoid having to enter each matrix, whenever a different cut is selected, it is much simpler to use the constants for quartz at a standard orientation, which is already included in COMSOL, and perform the cut rotation using the software. As an example, the left-handed quartz matrix constants are presented in the Table 3. The matrices has some symmetries because, quartz belongs to the trigonal crystal system.

Simulation times are quite long, and may be difficult to find the desired resonances, as *c* in Equation 4 is changing. Equation 7 can be used to locate the resonance frequency, thus reducing the search time, by giving the frequency around which the simulation should be carried out.

$$f(\theta)=\frac{1}{2h}\sqrt{\frac{c_{66}\cos^2\theta+c_{44}\sin^2\theta+2c_{14}\sin\theta\cos\theta}{\rho}} \qquad (7)$$

## 3. Use of COMSOL Multiphycis

To simulate the quartz plate resonator, the approach was to perform initially in 2D simulations using the AT-cut matrices. This 2D simulation help to perform an exploration of the behavior of the electrical susceptance (imaginary part of the admittance) of the transducer. The plate deformation at different harmonics of the shear thickness mode was also investigated. With the 2D results, more detailed 3D simulations were carried out.

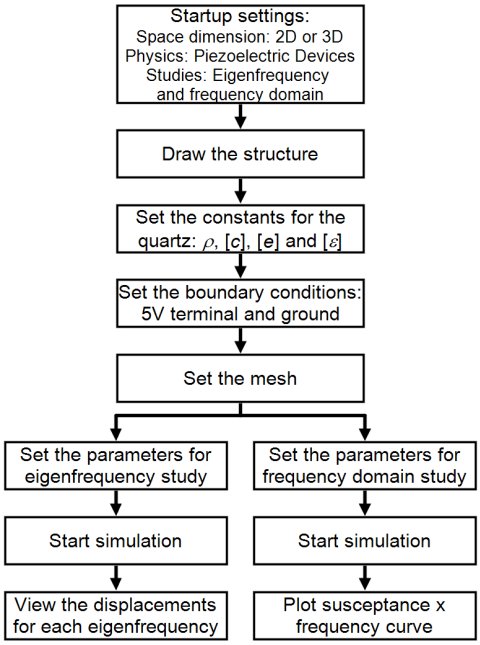


**Figure 4**. Flowchart for simulation of the quartz resonator.

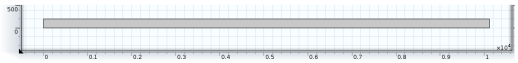

**Figure 5**. Geometry of the 2D quartz crystal plate resonator. The dimensions are 10115.28 × 200 µm.

The COMSOL Piezoelectric Devices interface combines Solid Mechanics and Electrostatics for modeling the piezoelectric devices. All or a subset of the domains may contain a piezoelectric material. The piezoelectric coupling can be on stress-charge or strain-charge form [11]. A step-by-step flowchart for the simulation is presented in Figure 4. Next, the 2D and 3D simulations are described in more detail.

### 3.1 2D simulations

The first step is to drawn the plate with a single domain (see Figure 5), with all boundaries mechanically free. For 2D simulations, only the AT-cut quartz constants were used. It is important to place the thickness direction along the y-axis for correct orientation of the AT-cut matrices, shown in Table 2. For this geometrical choice the deformations occur in the x-direction.

Electrodes are defined as the top and bottom lines, and an external AC signal is applied. One

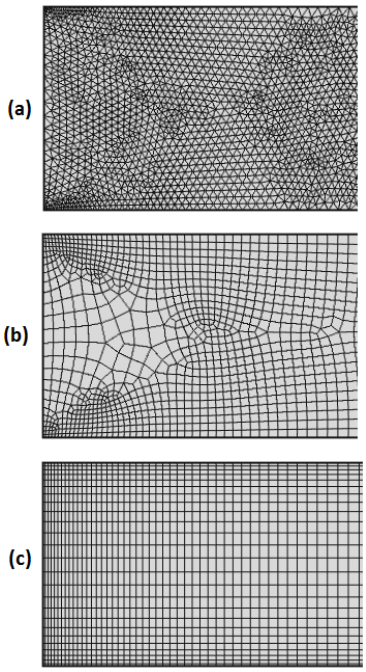


**Figure 6**. Types of mesh for 2D simulations: free triangular (a), free quadratic (b) and mapped (c).

electrode is set as the driving terminal and the voltage amplitude is set to 5 V. The other is set to ground. Next the mesh has to be define. For 2D simulation, three types of meshes can be constructed (see Figure 6): free triangular, free quadratic and mapped. It can be seen that there is a higher node concentration near the edges, this is achieved by adding an element ratio in a configuration type distribution. It was observed that for a given dimension the free quadratic and mapped meshes yield fewer number of elements, consequently a lower computational time, but no effect is observed in the harmonic frequency position, as compared with mapped mesh. Only for the mesh mapped, the number of elements can be pre-calculated, simply multiplying the number of elements in each edge. The mapped mesh was selected for 2D simulations. The mesh size is chosen to be at least ten times smaller than the fifth harmonic wavelength. For this work, the mesh was generated with 100 x 25 finite elements.

### 3.2 3D simulations

The geometry for the 3D analysis can be viewed in Figure 7. A work plane is created using the general type, in this window, three points are

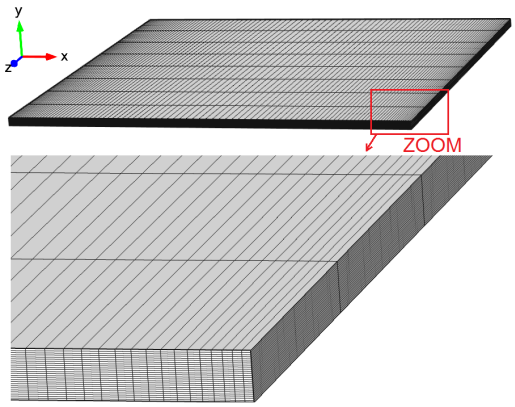


**Figure 7**. Geometry of the 3D quartz crystal plate resonator, a zoom-in is in the bottom. The dimensions are 10115.28 × 10115.28 × 200 µm.

| | x: | y: | z: |
|---|---|---|---|
| Point 1: | 0 | 0 | 0 |
| Point 2: | cos(phi*pi/180) | sin(phi*pi/180) | 0 |
| Point 3: | sin(phi*pi/180)*sin(tetha*pi/180) | -sin(tetha*pi/180)*cos(phi*pi/180) | cos(tetha*pi/180) |

**Figure 8**. The work plane is defined by the angles $\theta$ and $\varphi$.

defined as presented in Figure 8, the $\theta$ and $\varphi$ parameters can be easily changed for the selected cut (see Figure 1). Then an extrude operation is performed up to the desired thickness. For this work, the constants of the left-handed quartz are used (Table 3). By modifying the angles in the work plane window, one can explore other cuts with single and double rotations. The thickness direction must be along the y-axis for correct orientation. The mapped type mesh with 100 x 25 finite elements are defined in the surface parallel to the xy-plane and then a swept is carried out for 8 transversal planes to the z-axis, resulting in 20000 finite elements. The results are analyzed in the post-processing mode and will be discussed in the next section.

## 4. Results and analysis

Studies are performed in the eigenfrequency modes and frequency domain, and the results are analyzed in the post-processing mode. For this work, a computer with a ASUS P6T7 supercomputer motherboard with 8-core Intel i7, and 24 GB RAM was used.

### 4.1 2D simulations

In this work, the plate was designed with a thickness h = 200 µm and for m = 31 in

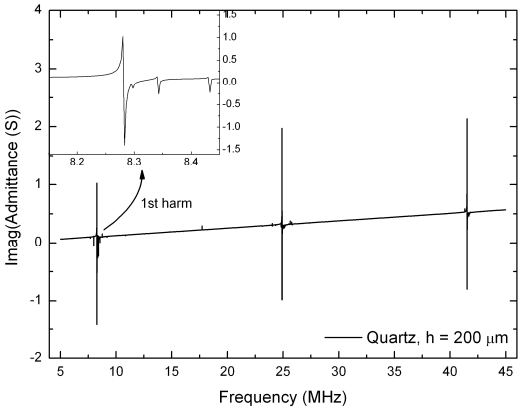


**Figure 9**. Imaginary part of the admittance for 2D simulations with the AT-cut quartz constants.

**Table 4:** Results for 2D simulations with the AT-cut quartz constants.

| harmonic | frequency (MHz) | | relative error (%) |
|---|---|---|---|
| | theory | COMSOL | |
| $f_1$ | 8.3054 | 8.2852 | 0.244 |
| $f_3$ | 24.9163 | 24.9103 | 0.024 |
| $f_5$ | 41.5272 | 41.5365 | 0.022 |

Equation 6, one can calculated a = 10115.28 µm. For the AT-cut quartz constants, $k_{26}^2 = 0.78$ % and $\hat{c}_{66} = 29.24 \times 10^9$ N/m$^2$, for $\rho = 2649$ kg/m$^3$, so v = 3322 m/s.

To evaluate the BAW resonator, one typically measures the complex impedance or the complex admittance as a function of frequency. Such quantities can be extracted from the simulation. The simulations were performed with standard settings for the solvers in the 5 MHz to 45 MHz frequency range, with a step of 10 kHz near of the resonances. In Figure 9, a plot of the imaginary part of the admittance that covers from first to fifth harmonic is presented. A comparison between theoretical and simulated harmonics is shown in Table 4, it shows a good agreement especially for higher harmonics.

It can be seen in Figure 9 that others resonances also appear. However, by observing the deformation shape, one can see that it is not related to the shear thickness mode and in most cases are spurious modes. In order to verify this observation a second study of eigenfrequencies was performed. The displacement shapes in the vicinities of the 1st, 3rd and 5th harmonics are analyzed and the results are shown in Figure 10, blue and red colors correspond to displacements in opposite directions. The plate displacement in

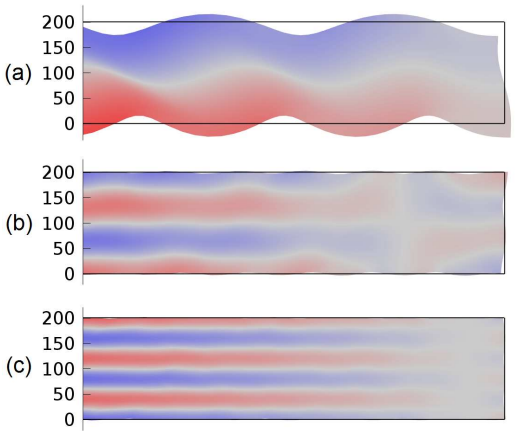


**Figure 10**. Displacements field (x-component) in 2D simulation, the shear thickness mode are presented. (a) Fundamental harmonic, (b) third harmonic and (c) fifth harmonic. The scale factor is 50000.

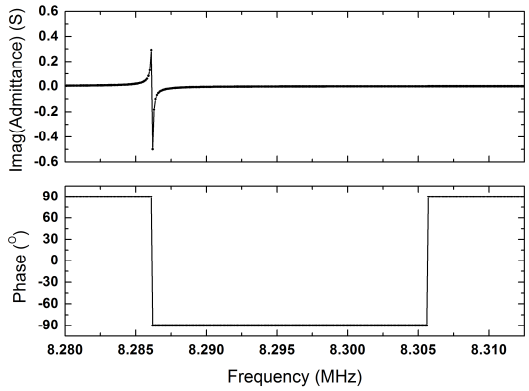


**Figure 11**. Imaginary part of the admittance and phase for the first harmonic for 3D simulation using the left handed quartz constants with θ = 35.25° and φ = 0°. A step of 100 Hz is performed. A simulation time of 4 hours is required.

the figure is highly amplified for observation. It can be see for the 3rd and 5th harmonics the presence of nodes at the plate end, it was not possible to isolate only the shear thickness mode in the simulation, so there appear some displacements in the horizontal boundaries, but the sinusoidal shape in the vertical boundaries is observed for all harmonics as expected.

### 4.2 3D simulations

The 3D simulation follows the same steps as for 2D, except that the left handed quartz constants (Table 3) are used. Now, the computational effort is much higher and the simulation was

**Table 5:** Results for 3D simulations with the left handed quartz constants.

| θ (°) | cut | frequency (MHz) | | | |
|---|---|---|---|---|---|
| | | theory | COMSOL | | |
| | | $f_1(\theta)$ | $f_1$ | $f_3$ | $f_5$ |
| -60 | BC | 12.7532 | 12.7595 | 38.2878 | 63.8457 |
| -57 | FT | 12.7541 | 12.7605 | 38.2962 | 63.8461 |
| -49 | BT | 12.6573 | 12.6664 | 38.0314 | 63.3996 |
| 31 | AC | 8.2513 | 8.2650 | 24.8696 | 41.4638 |
| 35.25 | AT | 8.2736 | 8.2855 | 24.9105 | 41.5292 |
| 38 | CT | 8.3211 | 8.3318 | 25.0377 | 41.7396 |
| 42.75 | ST | 8.4616 | 8.4723 | 25.4359 | 42.4009 |
| 66.5 | ET | 9.9510 | 9.9539 | 29.8555 | 49.7641 |

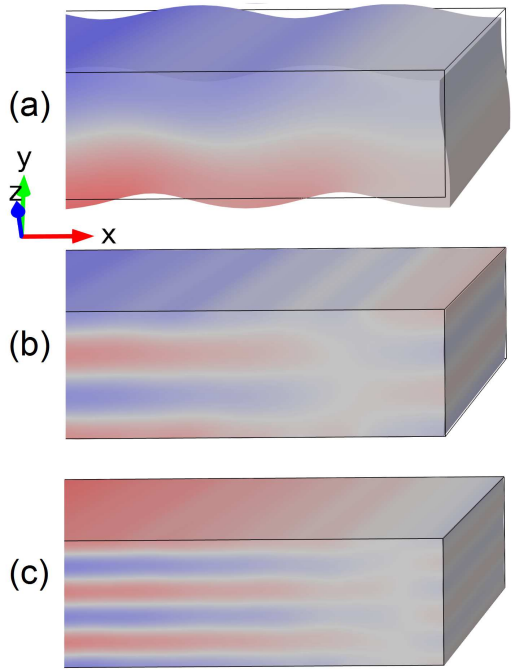


**Figure 12**. Displacement field (x-component) for the first (a), third (b) and fifth (c) harmonics in 3D simulation for the left handed quartz constants with θ = 35.25° and φ = 0°, the shear mode are presented. The scale factor is 30000.

only was carried out around the first harmonic, the behavior of the imaginary part of the admittance and phase is shown in Figure 11. The results are summarized in the Table 5. The displacements can be seen in the Figure 12. Again, there occurs other vibration modes as found in 2D.

Using the AC/DC module, an electrostatic study was performed to obtain the static capacitance of the plate. The basic parallel plate expression in Equation 8 yields the capacitance

of 20.059618 pF. The simulation resulted in a capacitance of 20.069107 pF, a very good agreement.

$$C_0 = \frac{\varepsilon_{22} a^2}{h} \tag{8}$$

After, this a parameter extraction for the equivalent circuit model was carried out. From the plot in Figure 11 and using an appropriate extraction algorithm, the values obtained are C = 94.083282 fF, L = 3.921181 mH and R = 2.003140 Ω. The quality factor could be calculated according to the Equation 9, Q = 101915.66. This value is a simulation artifact, since no damping was inserted in the simulation, hence the value of R should be zero. This can be verified by reducing the simulation step. The simulation step should be small enough for the damping to determine the losses.

$$Q = \frac{\omega_s}{\Delta\omega_{3dB}} = \frac{1}{R}\sqrt{\frac{L}{C}} \tag{9}$$

## 5. Conclusions

Quartz is an anisotropic piezoelectric material. Its physical constants changes with orientation. With COMSOL, this anisotropic behavior can be studied. 2D and 3D BAW quartz resonators were simulated, with different cuts. In 2D simulations, different types of mesh were analyzed, and the shorter calculation time helped explore wider frequency ranges. For the 2D simulation, the mapped mesh yields the same result as the other mesh types, but had the advantage of reduced computational time. Thin AT-cut quartz plate has been simulated and the resonances frequencies up to fifth harmonics were compared with theory, observing less than 0.3 % errors.

In 3D analysis mode, single and double rotation were performed to get the desired cut. For the simulation, the constants for the left handed quartz was used. In the specific AT-cut with $\theta = 35.25°$ and $\varphi = 0°$, the results are in good agreement with the 2D simulations. It was shown that the displacements occurred in the x-direction, and that the shear thickness vibration mode and others modes are presented.

Next, the damping will be included in the simulation to get correct equivalent circuit parameters and quality factor. There is also interest in evaluating the effect of the electrodes on the transducer, and analyze other 3D structures. With COMSOL, it expected to save design time before performing the actual maching of the quartz blank.

## 6. References


1. R. Weigel, D. Morgan, J. Owens, A. Ballato, K. Lakin, K. Hashimoto, and C. Ruppel, Microwave Acoustic Materials, Devices, and Applications, *IEEE Transactions on Microwave Theory and Techniques*, **50**, no. 3, 738–749 (2002).
2. K. Lakin, A Review of Thin-Film Resonator Technology, *IEEE Microwave Magazine*, **4**, no. 4, 61–67 (2003).
3. M. Weihnacht, Links between temperature stable baw and saw crystal orientations, *IEEE in Ultrasonics Symposium*, **2**, 914–917 (2005).
4. G. Kirikera, W. Patton, and S. Behr, Modeling Thickness Shear Mode Quartz Sensors for Increased Downhole Pressure & Temperature Applications, *Proceedings of the COMSOL Conference 2010 Boston*.
5. B. N. Johnson and R. Mutharasan, The Origin of Mass-change Sensitivity within Piezoelectrically-actuated Millimeter-sized Cantilever (PEMC) sensors: Vibrational Analysis through Experiment and Finite Element Modeling, *Proceedings of the COMSOL Conference 2009*.
6. L. Spicci and M. Cati, Ultrasound Piezo-Disk Transducer Model for Material Parameter Optimization, *Proceedings of the COMSOL Conference 2010 Paris*.
7. M. Patel, Y. Yong, and M. Tanaka, Drive Level Dependency in Quartz Resonators, *International Journal of Solids and Structures*, **46**, no. 9, 1856–1871 (2009).
8. C. Zhang, N. Liu, J. Yang, and W. Chen, Thickness-Shear Vibration of AT-Cut Quartz Plates Carrying Finite-Size Particles With Rotational Degree of Freedom and Rotatory Inertia [Correspondence], *IEEE Transactions on Ultrasonics, Ferroelectrics and Frequency Control*, **58**, no. 3, 666–670 (2011).
9. J. Wang and W. Zhao, The determination of the optimal length of crystal blanks in quartz crystal resonators, *IEEE Transactions on Ultrasonics, Ferroelectrics and Frequency Control*, **52**, no. 11, 2023–2030 (2005).
10. J. Yang, *Analysis of piezoelectric devices*. World Scientific (2006).
11. COMSOL Multiphysics 4.2a documentations.


## 7. Acknowledgements


The authors thanks PETROBRAS-GEDIG research network for the support. PETROBAS is the Brazilian oil company.